JBC RESEARCH ARTICLE

Exosomal miR-23a-3p derived from human umbilical cord mesenchymal stem cells promotes remyelination in central nervous system demyelinating diseases by targeting Tbr1/Wnt pathway

Received for publication, July 26, 2023, and in revised form, October 26, 2023 Published, Papers in Press, November 22, 2023,
https://doi.org/10.1016/j.jbc.2023.105487

Danqing Qin[1], **Chunjuan Wang**[1,2], **Dong Li**[1], **and Shougang Guo**[1,2,*]

From the [1]*Department of Neurology, Shandong Provincial Hospital, Cheeloo College of Medicine, Shandong University, Jinan, China;* [2]*Department of Neurology, Shandong Provincial Hospital, Shandong First Medical University, Jinan, China*

Reviewed by members of the JBC Editorial Board. Edited by Qi-Qun Tang

Oligodendrocyte precursor cells are present in the adult central nervous system, and their impaired ability to differentiate into myelinating oligodendrocytes can lead to demyelination in patients with multiple sclerosis, accompanied by neurological deficits and cognitive impairment. Exosomes, small vesicles released by cells, are known to facilitate intercellular communication by carrying bioactive molecules. In this study, we utilized exosomes derived from human umbilical cord mesenchymal stem cells (HUMSCs-Exos). We performed sequencing and bioinformatics analysis of exosome-treated cells to demonstrate that HUMSCs-Exos can stimulate myelin gene expression in oigodendrocyte precursor cells. Functional investigations revealed that HUMSCs-Exos activate the Pi3k/Akt pathway and regulate the Tbr1/Wnt signaling molecules through the transfer of miR-23a-3p, promoting oligodendrocytes differentiation and enhancing the expression of myelin-related proteins. In an experimental autoimmune encephalomyelitis model, treatment with HUMSCs-Exos significantly improved neurological function and facilitated remyelination. This study provides cellular and molecular insights into the use of cell-free exosome therapy for central nervous system demyelination associated with multiple sclerosis, demonstrating its great potential for treating demyelinating and neurodegenerative diseases.

Multiple sclerosis (MS) is the predominant autoimmune disorder affecting the central nervous system (CNS), which is the main cause of neurologic dysfunction in young people and has a high disability rate (1). MS is characterized by demyelination of the CNS, and myelin loss may be the result of immune-mediated processes or dysfunction of myelin-forming oligodendrocytes (OLs) (2). Axonal damage caused by the breakdown of myelin can lead to nerve conduction defects, resulting in severe sensory and motor symptoms (3). It has been suggested that the migration and differentiation of oligodendrocyte progenitor cells (OPCs) are decisive factors in promoting the regeneration of myelin in MS lesions. However, the gradual depletion of OPCs during the process of chronic demyelination hinders axonal remyelination (4). To overcome the lack of remyelination, there is an urgent need for emerging therapeutic approaches to activate OPCs and promote their differentiation into mature myelin-producing OLs, addressing this challenging issue.

Mesenchymal stem cells (MSCs) are multipotent progenitor cells that promote tissue regeneration and modulate neuroinflammation (5). Several studies have shown that MSCs can reduce neuroinflammation, improve neurological recovery, and regulate myelin regeneration and have gradually emerged as potential therapeutic tools for CNS demyelinating diseases (6, 7). Compared to other sources of stem cells, human umbilical cord mesenchymal stem cells (HUMSCs) offer distinct advantages, including affordability, ease of procurement, and adaptability (8). They typically exert beneficial effects on regeneration and repair in the form of paracrine secretion. In recent years, MSCs-derived exosomes (MSCs-Exos) have received extensive attention. These single-layered vesicles with diameters ranging from 40 to 150 nm transport various bioactive substances (such as DNA, microRNA, lipids, and proteins) between cells and are considered effective delivery vehicles and therapeutic targets (9). More importantly, exosomes can easily traverse the blood–brain barrier, which sets them apart in the treatment research of MS and other neurological diseases (10). For example, exosomes derived from human adipose-derived mesenchymal stem cells can effectively improve neurological deficits and promote myelin regeneration in mice with experimental autoimmune encephalomyelitis (EAE) through immunomodulatory effects (11). However, whether MSC-Exos can induce the differentiation of OPCs into myelinated OLs is still unclear.

In this work, we demonstrated the regulatory effect of HUMSCs-Exos on key cells, OLs, involved in myelinogenesis in MS. This effect is primarily mediated through the transfer of miR-23a-3p *via* exosomes, resulting in a significant inhibition of Tbr1 activity. It is worth noting that phosphoinositide 3-kinase (Pi3k)/Akt and Wnt signal pathway are also involved in the regulation of miR-23a-3p.

* For correspondence: Shougang Guo, guoshougang1124@163.com.

Results

Characteristics of HUMSCs-Exos

We isolated HUMSCs-Exos from the cell supernatants of cultured HUMSCs using a series of ultracentrifugation steps (Fig. 1*A*). Western blotting confirmed the positive expression of CD9, CD81, and TSG101 in HUMSCs-Exos, while they were not expressed in HUMSCs or in the culture medium without HUMSCs (Fig. 1*B*). The morphology, size, and quantity of HUMSCs-Exos were assessed using transmission electron microscopy (TEM) and nanoparticle tracking analysis (NTA), respectively. TEM images revealed that the HUMSCs-Exos exhibited characteristic round and oval-like structures (Fig. 1*C*). NTA results indicated that the concentration and particle size of the isolated HUMSCs-Exos ranged from 30 to 200 nm, with an average size of 142.5 nm (Fig. 1*D*). These findings demonstrate that the HUMSCs-Exos obtained in our experiments possess typical exosomal characteristics.

HUMSCs-Exos promote OPCs differentiation in vitro

As shown in Fig. 2*A*, immunofluorescent staining for NG2 and platelet-derived growth factor receptor α was performed to label OPCs, confirming a cell purity above 90%. PKH67-stained exosomes were cocultured with primary OPCs for 48 h, and the results demonstrated successful uptake of HUMSCs-Exos by recipient cells (Fig. 2*B*). Subsequently, using Western blotting (Fig. 2, *C* and *D*) and quantitative PCR (qPCR) (Fig. 2*E*), we examined the expression levels of classical differentiation markers in OPCs when treated with varying concentrations of HUMSCs-Exos. These markers included myelin-associated glycoprotein (Mag), myelin oligodendrocyte glycoprotein (Mog), and myelin basic protein (Mbp). Among them, there were no significant differences in Mag, Mog, and Mbp expression between OPCs treated with 3 μg/ml HUMSCs-Exos and the control group. However, when the concentration exceeded 12.5 μg/ml, their expression increased in OPCs after HUMSCs-Exos treatment. Especially in OPCs treated with high concentrations of HUMSCs-Exos (50 μg/ml, 100 μg/ml), the expression of Mbp, Mag, and Mog was significantly higher than in the low concentration group (3 μg/ml, 12.5 μg/ml), indicating a dose-dependent effect of HUMSCs-Exos on OPCs differentiation and maturation. Therefore, in subsequent investigations, we opted for a concentration of 50 μg/ml of exosomes as the optimal dosage for promoting OPCs differentiation toward mature OLs with myelin formation. Immunofluorescence analysis demonstrated an enhanced expression of Mbp in cells treated with HUMSCs-Exos (50 μg/ml, 48 h) compared to the control group (Fig. 2*G*).

It is worth noting that our study also revealed that HUMSCs-Exos at different concentrations exerted an inhibitory effect on apoptosis in OPCs (Fig. 2*F*). The expression of Bcl-2, similar to the differentiation markers, showed no significant difference between the OPCs treated with 3 μg/ml

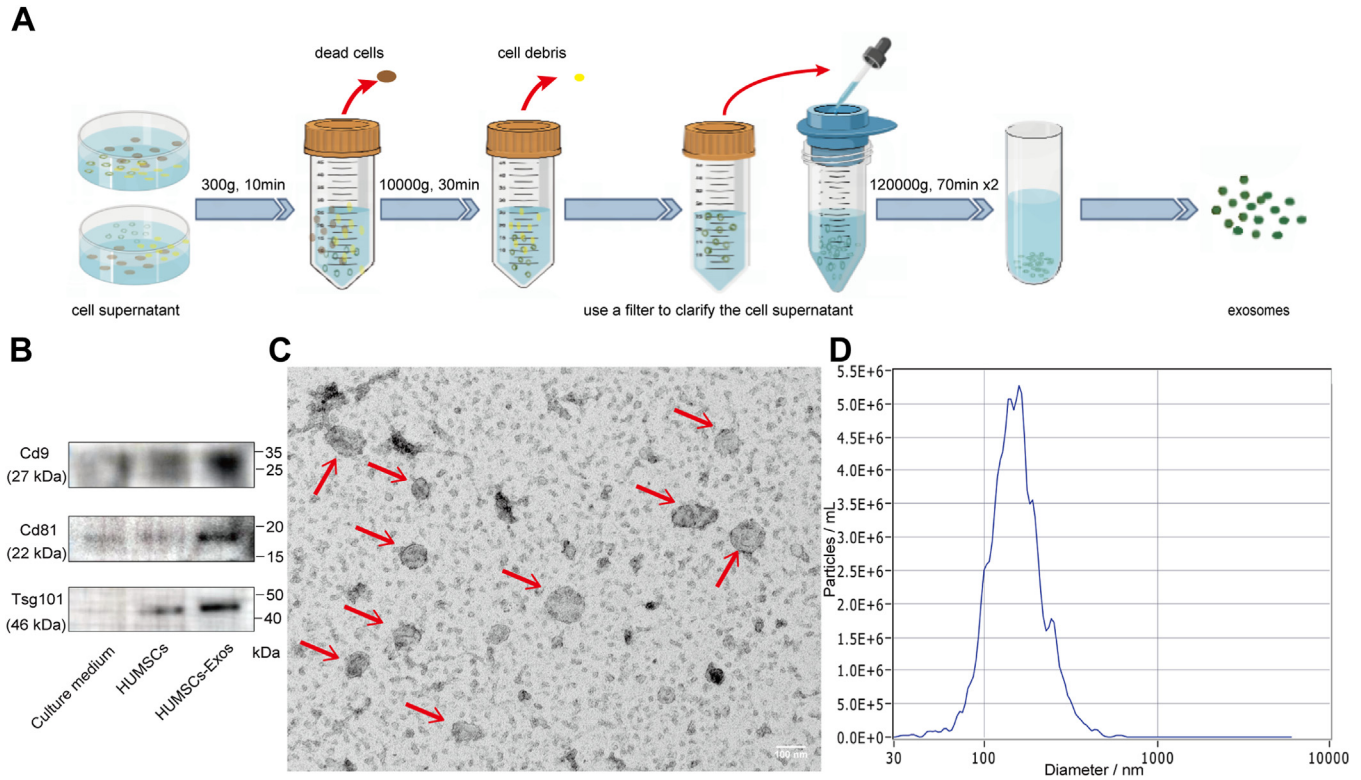

Figure 1. Isolation and characterization of HUMSCs-Exos. *A*, isolation process of HUMSCs-Exos. *B*, Western blotting results demonstrate positive expression of Cd9, Cd81, and Tsg101 in HUMSCs-Exos. *C*, morphological image of HUMSCs-Exos under TEM, the *red arrow* points to the circular or oval-shaped exosome. Scale bar: 100 nm. *D*, NTA analysis reveals that the peak size of HUMSCs-Exos is approximately 142.5 nm. HUMSCs-Exos, exosomes derived from human umbilical cord mesenchymal stem cells; NTA, nanoparticle tracking analysis; TEM, transmission electron microscopy.

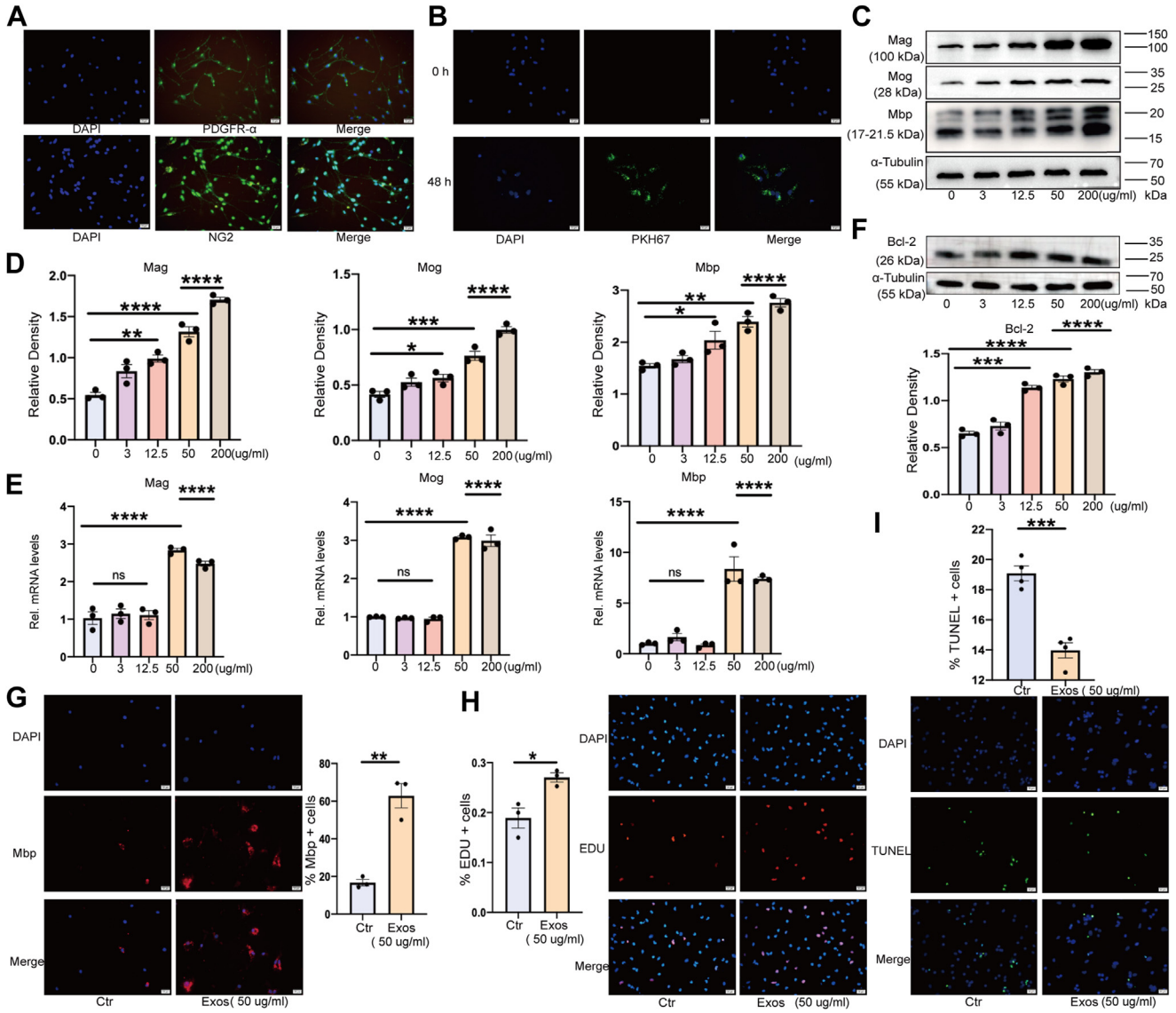

Figure 2. HUMSCs-Exos promote OPC maturation, differentiation, and myelin protein expression while inhibiting cell apoptosis. Purified primary rat OPCs were treated with HUMSCs-Exos. *A*, immunofluorescence staining of primary OPCs showing more than 90% of cells positive for NG2 and PDGFR-α (n = 3 per group). Scale bar: 20 μm. *B*, fluorescence image of PHK67-labeled HUMSCs-Exos cocultured with OPCs. Scale bar: 20 μm. *C* and *D*, Western blotting results and quantitative analysis of Mag, Mog, and Mbp (n = 3 per group). *$p < 0.05$, **$p < 0.01$, ***$p < 0.001$, ****$p < 0.0001$. *E*, qPCR analysis of Mag, Mog, and Mbp (n = 3 per group). ****$p < 0.0001$. *F*, Western blotting results and quantitative analysis of Bcl-2 (n = 3 per group). ***$p < 0.001$, ****$p < 0.0001$. *G*, representative images and percentage of Mbp-positive cells in HUMSCs-Exos–treated group (50 μg/ml) compared to the control group (n = 3 per group). Scale bar: 20 μm. **$p < 0.01$. *H*, representative images and proliferation rate of EDU-positive cells in the HUMSCs-Exos–treated group (50 μg/ml) compared to the control group (n = 3 per group). Scale bar: 20 μm. * $p < 0.05$. *I*, representative images and apoptotic rate of TUNEL-positive cells in the HUMSCs-Exos treated group (50 μg/ml) compared to the control group (n = 4 per group). Scale bar: 20 μm. ***$p < 0.001$. PDGFR-α, platelet-derived growth factor receptor α; HUMSCs-Exos, exosomes derived from human umbilical cord mesenchymal stem cells; OPC, oligodendrocyte progenitor cell; Mag, myelin-associated glycoprotein; Mog, myelin oligodendrocyte glycoprotein; Mbp, myelin basic protein; qPCR, quantitative PCR.

HUMSCs-Exos and the control group. However, when the exosome concentration exceeded 12.5 μg/ml, the expression of Bcl-2 significantly increased. This conclusion was further supported by TUNEL staining (Fig. 2*I*). In addition, EDU staining demonstrated that the exosome-treated group promoted cell proliferation compared to the control (Fig. 2*H*). These results collectively suggest that HUMSCs-Exos promote the proliferation and differentiation of OPCs into mature myelin-forming OLs while also inhibiting cell apoptosis *in vitro*.

HUSMC-Exos facilitate the development of mature myelinated OLs by delivering miR-23a-3p to modulate the Pi3k/Akt and Wnt pathways

To investigate the underlying mechanism by which HUMSCs-Exos promote the development of mature myelinated OLs, we employed full-length transcriptome sequencing technology to analyze the mRNA expression levels of OPCs treated with and without HUMSCs-Exos. This analysis identified a total of 824 significant differentially expressed genes (DEGs), with 687 DEGs upregulated and 137 DEGs downregulated

(fold change > 2, Q value < 0.05) (Fig. 3*A* and Table S1). To gain insights into the potential biological functions of these DEGs, we performed Gene Ontology enrichment and Kyoto Encyclopedia of Genes and Genomes pathway analysis. The results revealed significant upregulation of the Pi3k/Akt signaling pathway, phosphatidylinositol signaling system, and Mapk signaling pathway following HUMSCs-Exos treatment of OPCs (Fig. 3*B* and Table S1). Conversely, OLs differentiation, myelin sheath, and Wnt signaling pathways showed significant downregulation (Fig. 3*C* and Table S1). As shown in Fig. 3, *D* and *E*, the elevated levels of phosphorylated Akt (p-Akt) in OLs treated with HUMSCs-Exos, compared to the control group, confirm the activation of the PI3K/Akt pathway. The total Akt protein expression remains unchanged. Furthermore,

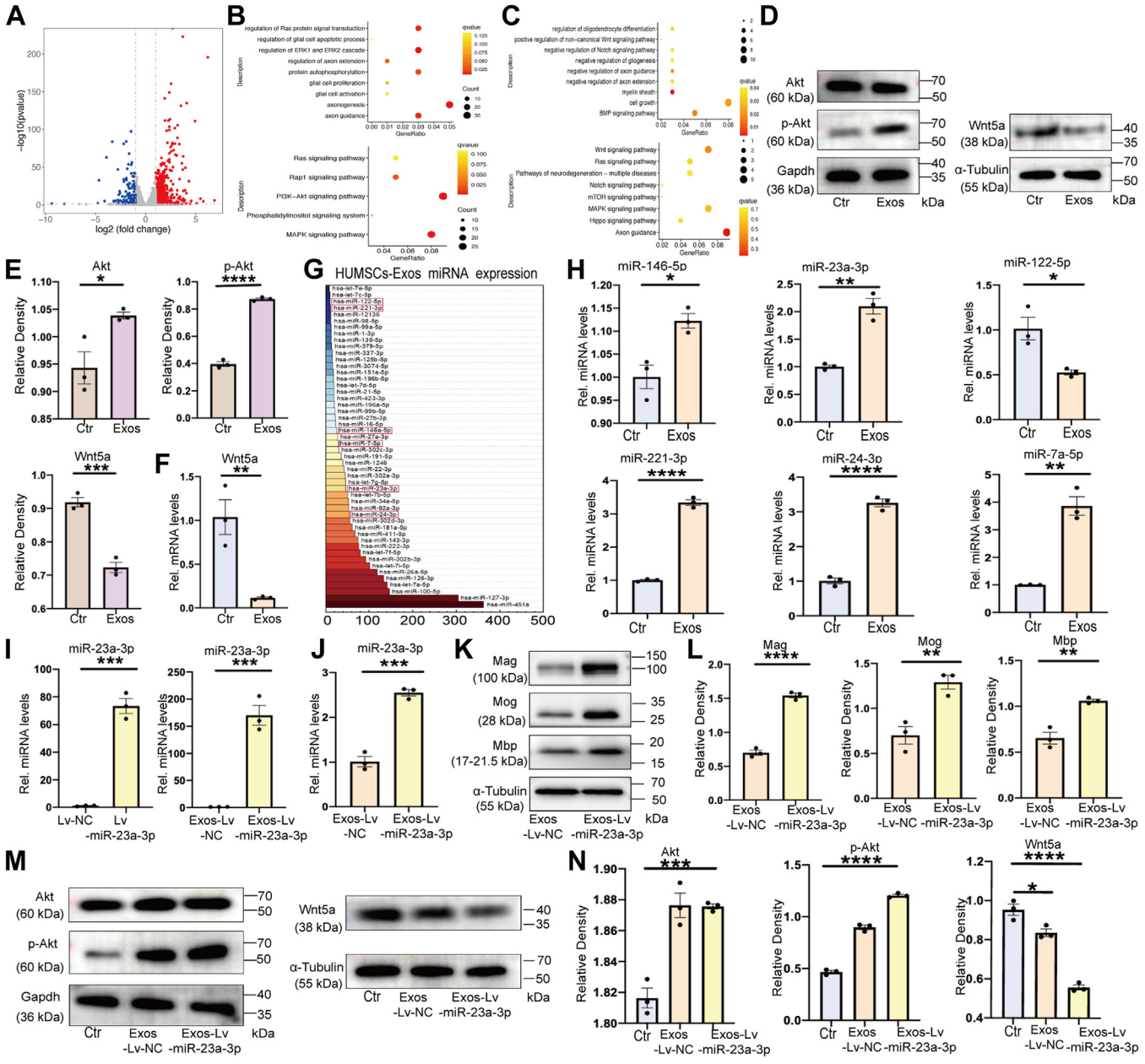

Figure 3. Promotion of OPC differentiation and maturation by HUMSCs-Exos *via* delivery of miR-23a-3p. *A*, volcano plot of differentially expressed genes (DEGs) between HUMSCs-Exos-treated and untreated OPCs. *Blue dots* represent downregulated DEGs, *red dots* represent upregulated DEGs, and *gray dots* represent nonsignificant DEGs. *B* and *C*, classification of DEGs based on KEGG pathway enrichment analysis and GO biological process annotation from the GO database. KEGG, Kyoto Encyclopedia of Genes and Genomes. GO, Gene Ontology. *D* and *E*, Western blotting analysis of Wnt5a, Akt, and p-Akt in OPCs Stimulated by HUMSCs-Exos (n = 3 per group). *$p < 0.05$, ***$p < 0.001$, ****$p < 0.0001$. *F*, qPCR measurement of Wnt5a expression in HUMSCs-Exos treated OPCs (n = 3 per group). **$p < 0.01$. *G*, the top 50 miRNAs identified in HUMSCs-Exos. *H*, qPCR analysis of myelin-associated miRNAs in OPCs treated with HUMSCs-Exos (n = 3 per group). *$p < 0.05$, **$p < 0.01$, ****$p < 0.0001$. *I*, qPCR detection of miR-23a-3p expression in HUMSCs and HUMSCs-Exos (n = 3 per group). ***$p < 0.001$. *J*, qPCR measurement of miR-23a-3p expression in OPCs (n = 3 per group). ***$p < 0.001$. *K* and *L*, Western blotting analysis of myelin-related proteins (Mag, Mog, and Mbp) in OPCs (n = 3 per group). **$p < 0.01$, ****$p < 0.0001$. *M* and *N*, Western blotting analysis of Wnt5a, Akt, and p-Akt proteins (n = 3 per group). ***$p < 0.001$, ****$p < 0.0001$. HUMSCs-Exos, exosomes derived from human umbilical cord mesenchymal stem cells; OPC, oligodendrocyte progenitor cell; Mag, myelin-associated glycoprotein; Mog, myelin oligodendrocyte glycoprotein; Mbp, myelin basic protein; qPCR, quantitative PCR.

stimulation by HUMSCs-Exos suppresses the levels of Wnt5a protein in OLs. qPCR results are consistent with the protein-level trends, demonstrating that HUMSCs-Exos inhibit the expression of Wnt5a (Fig. 3*F*).

Additionally, miRNA sequencing was performed on HUMSCs-Exos. Among the identified top 50 miRNAs, miR-146a-5p (12, 13), miR-23a-3p (14, 15), miR-122-5p (16, 17), miR-221-3p (18, 19), miR-24-3p (20), and miR-7a-5p (21, 22) were found to be closely associated with the myelin development (Fig. 3*G* and Table S2). qPCR data revealed significant upregulation of miR-23a-3p, miR-221-3p, and miR-24-3p in OPCs treated with HUMSCs-Exos compared to the untreated control group (Fig. 3*H*). Previous research has identified miR-23a-3p as a key regulatory factor promoting OPC differentiation and increasing myelin sheath thickness (14, 15), which suggested that miR-23a carried by HUMSCs-Exos might be involved in the development and maturation of OPCs. To further verify this hypothesis, we transfected HUMSCs with a lentiviral vector expressing miR-23a-3p (Lv-miR-23a-3p) and a negative control vector (Lv-NC). qPCR confirmed the significant upregulation of Lv-miR-23a-3p in both HUMSCs and HUMSCs-Exos, successfully obtaining HUMSCs-Exos overexpressing miR-23a-3p (Exos-Lv-miR23a-3p) (Fig. 3*I*). Subsequently, we cocultured modified HUMSCs-Exos (Exos-Lv-miR23a-3p) with OPCs for 48 h *in vitro*, and the results demonstrated that the expression of miR-23a-3p in Exos-Lv-miR23a-3p-treated OPCs was 2.5 times higher than in the Exos-Lv-NC-treated OPCs (Fig. 3*J*), indicating successful transfer of miR-23a-3p from HUMSCs-Exos to OPCs.

Western blotting further confirmed that the expression of myelin proteins (Mag, Mog, and Mbp) was significantly increased in OPCs treated with exos-lv-mir23a-3p compared to the NC (Exos-Lv-NC) group, demonstrating that HUMSCs-Exos delivered miR-23a-3p to promote OPC differentiation into mature myelinating OLs (Fig. 3, *K* and *L*). Furthermore, based on transcriptomic sequencing results, we detected the activation of the Pi3k/Akt pathway and inhibition of the noncanonical Wnt signaling molecule Wnt5a in OPCs following HUMSCs-Exos delivery of miR-23a-3p (Fig. 3, *M* and *N*). These findings collectively suggest that HUMSCs-Exos-delivered miR-23a-3p enhances myelin activity, promotes the development of mature myelinating OLs, and regulates the Pi3k/Akt and Wnt signaling pathways.

miR-23a-3p targets Tbr1 and Wnt signaling molecules to promote myelin formation

To further explore the mechanistic role of miR-23a in OPCs, we utilized the miRDB (http://mirdb.org/miRDB/index.html) and TargetScan (http://www.targetscan.org) databases to predict the downstream genes of miR-23a-3p. Biological analysis revealed that Tbr1 is a potential target gene of miR-23a-3p, as predicted by miRDB with a score higher than 80, and validated through cross-analysis with the cell transcriptomic mRNA sequencing of HUMSCs-Exos treatment (Tables S1 and S3). Next, the binding site between miR-23a-3p and Tbr1 was predicted using the TargetScan database (Fig. 4*A*). In order to confirm the interaction between miR-23a-3p and Tbr1, dual-luciferase reporter gene assay was performed. As shown in Fig. 4*B*, miR-23a-3p mimics significantly inhibited the luciferase activity of Tbr1-3′-UTR-WT, while the activity of Tbr1-3′-UTR-MUT was unaffected. Furthermore, to further validate Tbr1 as a target of miR-23a-3p in OPCs, we independently transfected OPCs with miR-23a-3p mimics and their corresponding NC (mimics-miR-23a-3p-NC) and detected the expression of Tbr1 using Western blotting (Fig. 4*C*). The results showed a significant reduction in the protein levels of Tbr1 in OPCs transfected with miR-23a-3p mimics. These findings indicate that miR-23a-3p directly targets and regulates the expression of Tbr1 in OPCs.

Subsequently, we evaluated the role of Tbr1 in OPCs development. Firstly, the Tbr1 overexpression vector was constructed. As shown in Fig. 4*D*, successful high expression of Tbr1 in OPCs was achieved. Furthermore, as the expression of Tbr1 increased, the levels of myelin-associated proteins (Mag, Mog, and Mbp) showed a negative correlation with it (Fig. 4, *E* and *F*), indicating that Tbr1 inhibits the maturation and differentiation of OLs. Next, OPCs were transfected with mimics-miR-23a-3p and its corresponding NC (mimics-miR-23a-3p-NC). Simultaneously, the constructed Tbr1 overexpression vector was transfected into cells that had already been transfected with miR-23a mimics (mimics-miR-23a-3p + Tbr1-OE), and an empty vector was used as the NC (mimics-miR-23a-3p + Tbr1-NC). qPCR (Fig. 4*G*) and Western blotting images (Fig. 4, *H* and *I*) confirmed the successful generation of OPCs with high expression of miR-23a-3p and Tbr1. Overexpression of miR-23a-3p in OPCs enhanced the expression of myelin proteins such as Mag, Mog, and Mbp (Fig. 4, *J* and *K*), indicating the promotion of OLs maturation by miR-23a-3p, consistent with previous findings. Conversely, high expression of Tbr1 in OPCs not only directly decreased the levels of myelin proteins but also potentially reversed the effect of promoting OLs maturation caused by overexpression of miR-23a-3p (Fig. 4, *J* and *K*). These results suggest that Tbr1 plays an inhibitory role in OLs maturation and may counteract the promoting effects of miR-23a-3p.

Furthermore, studies have reported that the Wnt signaling molecule Wnt7a/b is involved in Tbr1-associated diseases (23) and can rescue axonal defects caused by Tbr1 (24, 25). Wnt7a/b, as a direct target of Tbr1, has been shown to increase the number of OPCs and promote their differentiation into myelinating OLs (26–30). Moreover, Wnt5a, as a noncanonical Wnt signaling molecule, has been demonstrated to play a great role in OPCs development mediated by HUMSCs-Exos (31). As shown in the aforementioned Fig. 3, *M* and *N*, its expression decreases with the increased delivery of miR-23a-3p from HUMSCs-Exos to OPCs. Therefore, to evaluate the reciprocal regulation between Tbr1 and Wnt signaling molecules, we performed Western blotting on Tbr1-overexpressing OPCs. The results showed a significant decrease in the expression levels of myelinating OL-promoting Wnt 7a/b proteins in OPCs with high Tbr1 expression, while the expression of the myelination inhibitory factor Wnt5a was significantly increased (Fig. 4, *L* and *M*).

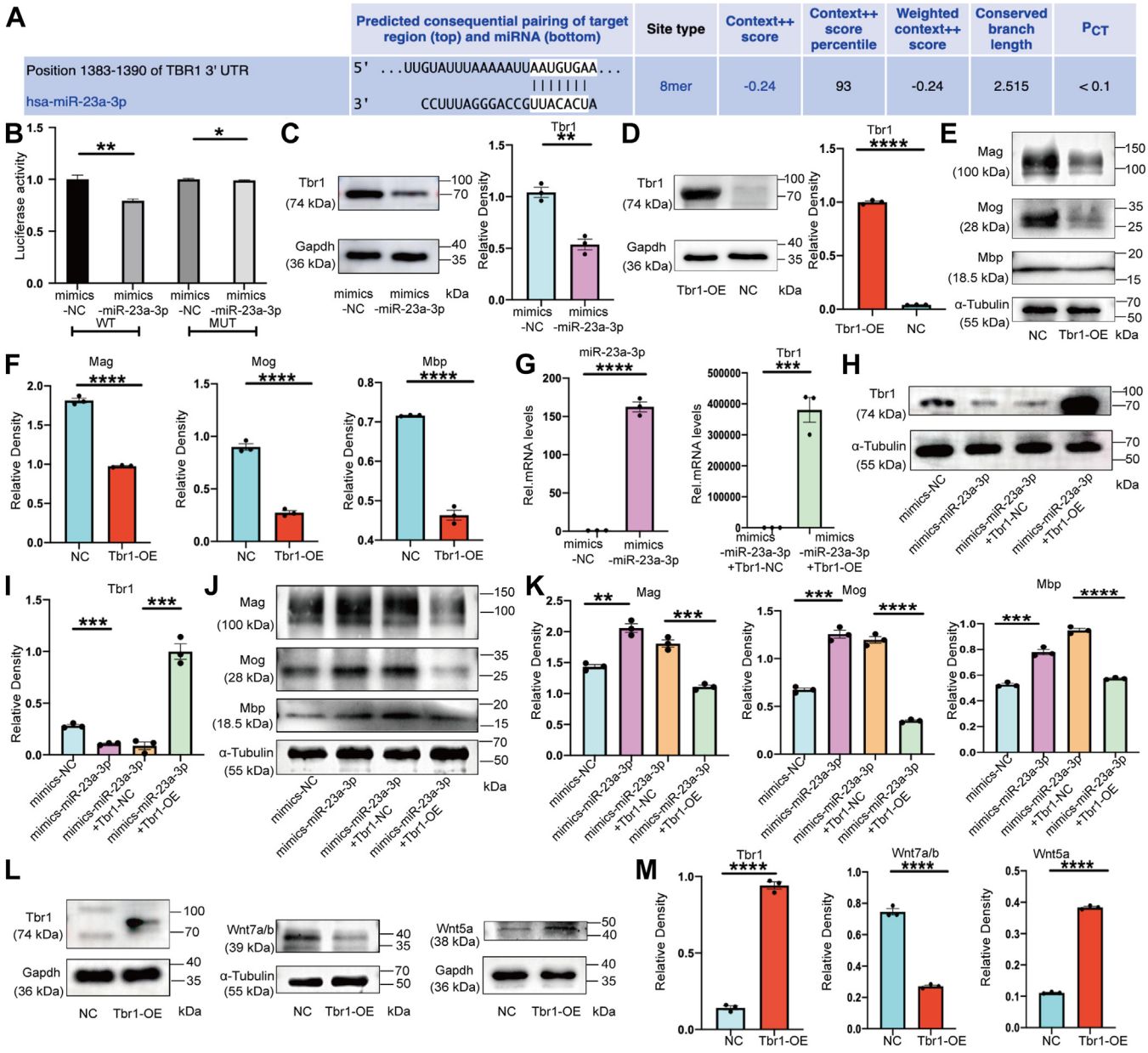

Figure 4. miR-23a-3p targets Tbr1 expression and evaluates the impact of Tbr1 on OLs development and maturation. *A*, predicted potential binding sites of miR-23a-3p in the 3′-UTR transcript of Tbr1 using TargetScan online tool. *B*, dual-luciferase reporter assay confirming the interaction between miR-23a-3p and Tbr1 3′-UTR (n = 3 per group). *$p < 0.05$, and **$p < 0.01$. *C*, Western blotting analysis of Tbr1 in OPCs transfected with mimics-miR-23a-3p and mimics-NC (n = 3 per group). **$p < 0.01$. *D*, Western blotting analysis of Tbr1 protein in OPCs (n = 3 per group). ****$p < 0.0001$. *E* and *F*, Western blotting images and analysis of myelin-related proteins (Mag, Mog, and Mbp) (n = 3 per group). ****$p < 0.0001$. *G*, qPCR detection of miR-23a-3p and Tbr1 expression levels (n = 3 per group). ***$p < 0.001$, ****$p < 0.0001$. *H* and *I*, Western blotting analysis of Tbr1 levels in cells transfected with mimics-NC, mimics-miR-23a-3p, mimics-miR-23a-3p + Tbr1-NC, and mimics-miR-23a-3p + Tbr1-OE (n = 3 per group). ***$p < 0.001$, ****$p < 0.0001$. *J* and *K*, Western blotting analysis of myelin-associated proteins (Mag, Mog, and Mbp) levels in cells transfected with mimics-NC, mimics-miR-23a-3p, mimics-miR-23a-3p + Tbr1-NC, and mimics-miR-23a-3p + Tbr1-OE (n = 3 per group). **$p < 0.01$, ***$p < 0.001$, and ****$p < 0.0001$. *L* and *M*, Western blotting detection of Tbr1, Wnt7a/b and Wnt5a proteins (n = 3 per group). ****$p < 0.0001$. OPC, oligodendrocyte progenitor cell; Mag, myelin-associated glycoprotein; Mog, myelin oligodendrocyte glycoprotein; Mbp, myelin basic protein; qPCR, quantitative PCR.

Application of exosome therapy in promoting myelin repair in EAE mouse model

In order to investigate the therapeutic effects of exosomes on remyelination in demyelinated mice with EAE, mice were immunized with the MOG (35–55) probe and injected with pertussis toxin to disrupt the blood-brain barrier. In the treatment group, HUMSCs-Exos (Exos-Lv-NC) and modified HUMSCs-Exos (Exos-Lv-miR23a-3p) were intravenously injected *via* the tail vein starting from day 15 (corresponding to the peak disease score), while the control group received phosphate-buffered saline (PBS) injections. Neurological function scores were assessed daily during the aforementioned period (Fig. 5*A*). Compared to untreated animals (PBS group), exosome treatment significantly delayed and attenuated the recurrence of disease symptoms, with the score of the modified HUMSCs-Exos (Exos-Lv-

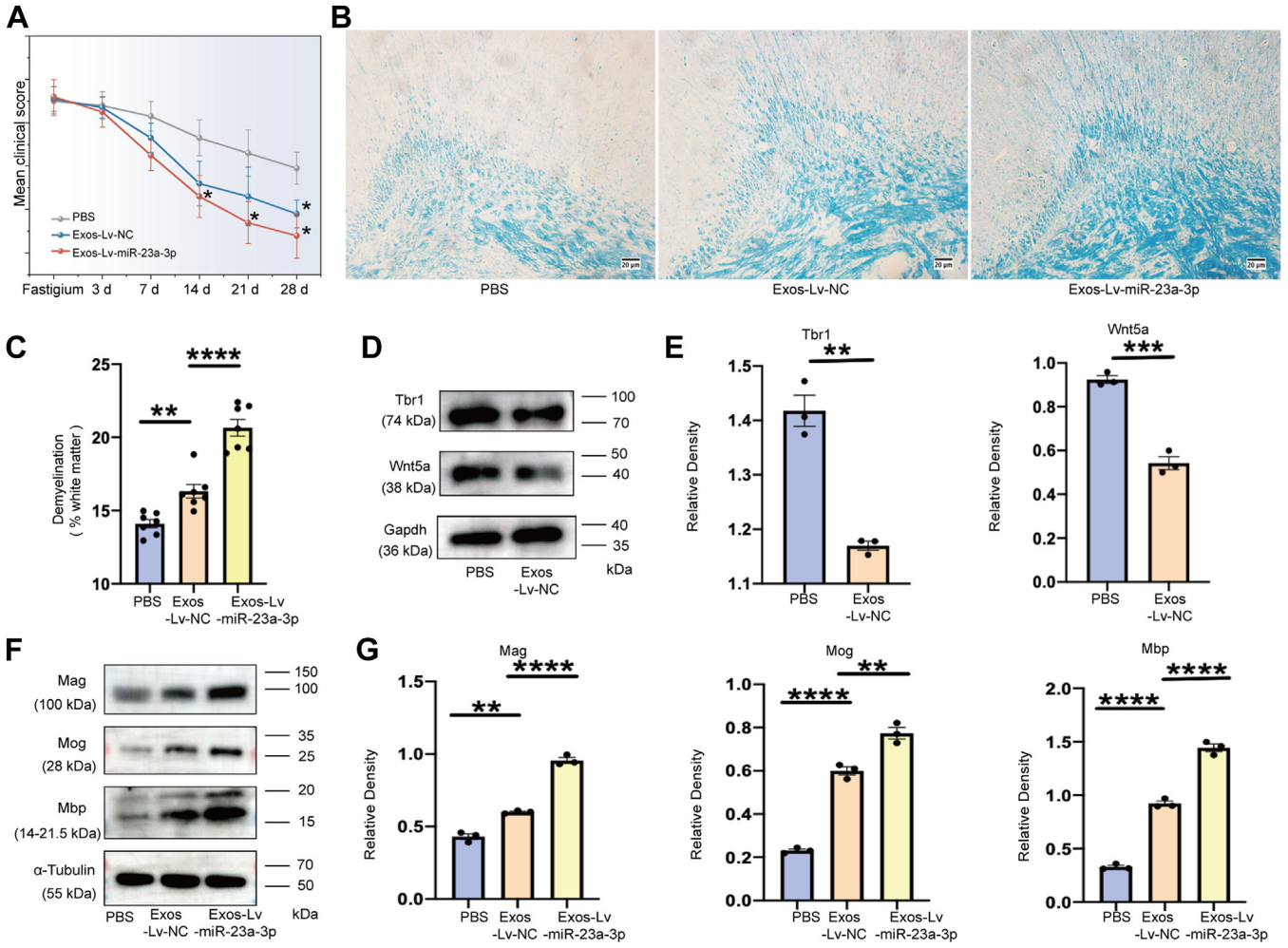

Figure 5. Exosomes promote remyelination in EAE mice. *A*, clinical neurological function scores of mice in the PBS group, HUMSCs-Exos (Exos-Lv-NC) group, and modified HUMSCs-Exos (Exos-Lv-miR-23a-3p) group during EAE (n = 10 per group). *$p < 0.05$. *B* and *C*, Luxol Fast Blue staining of brain sections to measure the demyelinated area and myelin staining intensity in the white matter (n = 7 per group). **$p < 0.01$, ***$p < 0.001$. *D* and *E*, Western blotting images and analysis of Tbr1 and Wnt5a levels in brain tissues (n = 3 per group). **$p < 0.01$, ***$p < 0.001$. *F* and *G*, Western blotting images and analysis of myelin-related proteins (Mag, Mog, and Mbp) in brain tissues (n = 3 per group). **$p < 0.01$, ****$p < 0.0001$. EAE, experimental autoimmune encephalomyelitis; HUMSCs-Exos, exosomes derived from human umbilical cord mesenchymal stem cells; Mag, myelin-associated glycoprotein; Mog, myelin oligodendrocyte glycoprotein; Mbp, myelin basic protein; PBS, phosphate-buffered saline.

miR23a-3p) group significantly lower than that of the HUMSCs-Exos (Exos-Lv-NC) group, approaching normal levels.

Subsequently, to assess the effect of exosomes on EAE-related CNS pathology, especially demyelination, white matter was taken from brains 14 days after tail vein injection (day 29). Brain tissue analysis revealed reduced demyelination in the treated animals compared to the untreated EAE group (PBS group). Demyelination was quantitatively assessed by evaluating Luxol fast blue (LFB) staining area using Image J software and subjected to statistical comparison. As shown in Fig. 5*C*, both the HUMSCs-Exos (Exos-Lv-NC) group and the modified HUMSCs-Exos (Exos-Lv-miR23a-3p) group significantly promoted remyelination after demyelination. When comparing the intensity of myelin staining within the lesions, we observed that the HUMSCs-Exos (Exos-Lv-NC) group exhibited higher myelin staining density and a larger area of blue-stained tissue compared to the PBS group. Similarly, the modified HUMSCs-Exos (Exos-Lv-miR23a-3p) group displayed a more concentrated and regular LFB staining pattern, indicating a significantly deeper myelin staining level (Fig. 5*B*).

Furthermore, as depicted in Figure 5, *D* and *E*, both the PBS group and the HUMSCs-Exos group exhibited alterations in the Tbr1/Wnt signaling pathway. Notably, HUMSCs-Exos treatment effectively reduced the expression of Tbr1 and Wnt5a, offering further insights into the potential benefits and mechanisms of action of HUMSCs-Exos in treating EAE mice. Western blotting analysis of myelin-associated proteins (Mag, Mog, and Mbp) also supported the conclusion that exosomes treatment may enhance myelin repair (Fig. 5, *F* and *G*). The exosome-treated group showed enhanced protein expression levels, with the modified HUMSCs-Exos (Exos-Lv-miR23a-3p) group exhibiting the most significant increase, suggesting that exosomes may exert their therapeutic effects through miR-23a-3p. In summary, exosome treatment delays the

recurrence of disease symptoms, reduces demyelination, and enhances myelin repair in EAE mice.

Discussions

MS, the most prevalent autoimmune neurological disease among young individuals, often results in demyelination and subsequent axonal degeneration, leading to significant clinical morbidity and disability for many patients (32). New therapeutic approaches are therefore urgently needed to improve the clinical outcome of such diseases. In this context, the present study highlights the beneficial effects of MSCs-Exos in the context of demyelination injuries (33). To gain insight into the underlying mechanisms responsible for these therapeutic effects, our findings demonstrate that HUMSCs-Exos facilitate the maturation of myelinated OLs through various mechanisms, including the inhibition of Tbr1 expression, modulation of the Wnt signaling molecule, and downstream effects on Pi3k/Akt phosphorylation. Additionally, we provide evidence that miR-23a-3p is enriched in HUMSCs-Exos and exerts regulatory effects on OPCs differentiation and the expression of myelin proteins by targeting Tbr1. These discoveries shed light on the molecular mechanisms involved in the regenerative potential of HUMSCs-Exos and offer promising avenues for the development of novel therapeutic strategies in demyelinating diseases.

As a cell-free therapy for various human diseases, MSCs have shown promising therapeutic effects in cellular and animal models related to MS, including the induction of mature myelinated OLs, improvement of cognitive function in demyelinated mice, and promotion of myelin repair (34, 35). It is now well-established that the majority of MSCs' biological effects are mediated through paracrine secretion of soluble factors and exosomes (36). Exosomes, as potent secretory components of MSCs, are enriched with proteins, nucleic acids, and other active substances, serving as vital vehicles for intercellular transport (37). Several recent studies have demonstrated that MSC-derived exosomes can enhance overall neurological recovery, attenuate neuroinflammation, and promote myelin repair by inducing M2 polarization of microglia or reducing the proliferation of reactive astrocytes (11, 38, 39). However, the potential impact of HUMSCs-Exos on the differentiation of OPCs into mature myelinated OLs during myelin regeneration has received limited attention. Our study provides robust evidence that highlights the close relationship between the therapeutic efficacy of HUMSCs-Exos and their ability to regulate the mature differentiation of myelinated OLs. These findings hold significant promise for the treatment of neurodegeneration and neuroinflammation associated with autoimmune demyelinating diseases.

miRNAs are a crucial component of exosomes and play a significant role in exosome-mediated intercellular communication (40). They exert their effects by binding to the 3′UTR of target mRNA in a complementary manner, resulting in the inhibition of protein translation. This process has substantial implications for cell proliferation, differentiation, and senescence (41). Therefore, the biological effects of exosomes on recipient cells are largely determined by the specific miRNAs they carry. Studies have identified certain miRNAs with high abundance in MSCs-Exos that possess unique immunomodulatory effects and are involved in myelin damage and regeneration associated with MS. Examples include miR-122 (42), miR-21 (42, 43), miR-146a (44), miR-24 (45), and miR-223 (45, 46). To investigate the impact of HUMSCs-Exos on OPC differentiation and maturation, we performed transcriptome sequencing to identify DEGs between HUMSCs-Exos-treated OPCs and untreated OPCs. Additionally, we analyzed the miRNA composition in HUMSCs-Exos using miRNA target databases and relevant bioinformatics approaches, ultimately identifying miR-23a-3p as a key candidate. Numerous studies have shown a close association between miR-23a-3p and CNS myelin formation (14, 15). In our study, we demonstrated that overexpressing miR-23a-3p in HUMSCs using a lentivirus-mediated system resulted in increased miR-23a-3p levels in HUMSCs-Exos, thus obtaining modified HUMSCs-Exos (Exos-Lv-miR-23a-3p). Moreover, compared to OPCs treated with control HUMSCs-Exos, modified HUMSCs-Exos (Exos-Lv-miR-23a-3p) significantly enhanced the production of myelinated OLs and the expression of myelin proteins. Furthermore, we evaluated myelin remodeling in EAE mice using neurological function scores and LFB staining and found that modified HUMSCs-Exos (Exos-Lv-miR-23a-3p) promoted myelin regeneration, increased myelin density, and subsequently enhanced neurological recovery in EAE mice.

The Pi3k/Akt pathway and the Wnt signaling pathway are closely interconnected signaling pathways that play vital roles in cell growth, proliferation, and survival. They are crucial in various aspects of OLs development, including OPCs proliferation, migration, survival, differentiation, and myelination (47). Activation of the Pi3k and Akt proteins through phosphorylation has been shown to promote widespread myelination in the CNS and enhance OPCs differentiation and maturation (48). Conversely, inhibition of these pathways can reduce the expression of myelin proteins and impede the development of myelinated OLs (49, 50). Wnt signaling comprises both canonical Wnt/β-catenin signaling and noncanonical Wnt signaling, with the latter triggering alternative signaling pathways independent of β-catenin (51). Wnt5a is a noncanonical Wnt ligand that has been implicated in various pathologies, including cancer and inflammatory diseases (52, 53). Previous studies have shown that activated microglia in EAE mice mediate neurodegeneration through increased expression of noncanonical Wnt signaling components, in which overexpression of Wnt5a affects demyelinating lesions in mice and plays a role in demyelinating pathogenesis (31, 54). However, there is a lack of related reports elucidating the specific effects of the noncanonical Wnt signaling pathway on OPCs maturation and development. In our study, we examined both the Pi3k/Akt and Wnt signaling pathways and observed that treatment with HUMSCs-Exos, as well as modified HUMSCs-Exos (Exos-Lv-miR-23a-3p), resulted in the activation of the Pi3k/Akt pathway and inhibition of Wnt5a. These findings provide valuable insights into the interplay between these signaling pathways and their influence on OPCs maturation and development.

The downstream targets of miR-23a-3p have been verified using various methods, including the miRDB software,

Targetscan database, dual-luciferase reporter gene assays, and other research reports. Among these targets is Tbr1, a transcription factor that plays a crucial role in the differentiation of glutamatergic cells (55). Previous studies have demonstrated that Tbr1 is involved in the regulation of glial cell formation and contributes to the generation of neural stem cells that differentiate into neurons and OPCs (56).

However, the direct involvement of Tbr1 in the maturation and development of OPCs into myelinated OLs has not been reported. Our data indicate that HUMSCs-Exos or miR-23a mimics negatively regulate Tbr1 expression in OPCs, and an excess of Tbr1 leads to reduced expression of mature myelin proteins in these cells. Importantly, the promoting effect of miR-23a-3p on myelin protein expression in OLs can be reversed by overexpressing Tbr1. Thus, Tbr1 may represent a potential target for the differentiation and maturation of OPCs into OLs mediated by miR-23a-3p. According to existing reports, the Wnt signaling pathway may impact the differentiation of early neural progenitor cells through the regulation of neural transcription factor expression, including Tbr1 (57). Specifically, Wnt7a/b, as a component of the canonical Wnt signaling pathway, promotes OPCs (26), while Wnt5a, as a noncanonical Wnt signaling pathway component, inhibits myelination (58, 59). In our study, we confirmed that the expression of Wnt5a increased and the expression of Wnt7a/b decreased in OPCs treated with excessive Tbr1, consistent with the inhibition of myelin protein expression resulting from Tbr1 overexpression. These findings suggest that Tbr1 may regulate the differentiation and maturation of OPCs through the Wnt signaling pathway.

We investigated the potential neurorestorative effect of HUMSCs-Exos on remyelination in MS and found a close association with the key factor miR-23a-3p in maintaining myelin integrity. This discovery offers a promising therapeutic strategy for demyelinating diseases, particularly by manipulating the expression of exosome-specific cargo, such as miR-23a-3p, to optimize treatment outcomes. However, there are certain limitations to our study. First, although miR-23a-3p is one of the most abundant miRNAs in HUMSCs-Exos and plays a role in the differentiation and maturation of OPCs through the Tbr1/Wnt and Pi3k/Akt signaling pathways, the contribution of other miRNAs remains to be investigated. Second, while our experiments strongly support the inhibition of Tbr1/Wnt and activation of Pi3k/Akt by miR-23a-3p in OPCs, further extensive *in vivo* validation of this mechanism is necessary. Lastly, the therapeutic potential of the proteins and other beneficial components present in MSCs-Exos in CNS demyelinating diseases should be explored in more detail. In conclusion, we believe that MSCs-Exos hold significant promise as a treatment modality for CNS demyelinating diseases, and their underlying mechanisms warrant further in-depth investigation in future studies.

Conclusions

HUMSCs-derived exosomes, enriched with miR-23a-3p, play a crucial role in regulating the Pi3k/Akt and Tbr1/Wnt signaling pathways. By enhancing the expression of myelin proteins in OPCs, these exosomes effectively promote the maturation and development of myelinated OLs, thereby facilitating myelin regeneration. Furthermore, this study delves into the underlying mechanism of action of HUMSCs-Exos in demyelinating diseases, contributing to a deeper understanding of their therapeutic potential. These findings present a promising therapeutic approach for the treatment of CNS demyelinating diseases associated with MS.

Experimental procedures

Cell culture and treatment of HUMSCs

HUMSCs used in this study were obtained from the Cell Bank of the Chinese Academy of Sciences. The cells were cultured in low-glucose Dulbecco's modified Eagle Medium (Gibco) supplemented with 10% fetal bovine serum (FBS; Gibco). FBS was ultracentrifuged at 4 °C (Sorvall 100SE ultracentrifuge) at 100,000*g* for 18 h to deplete exosomes. When the third to sixth passage of HUMSCs reached 40% confluency, the regular culture medium was replaced with 10% exosome-depleted FBS culture medium. After 48 h, the cell culture supernatant was immediately collected for exosome isolation or stored at −80 °C.

Isolation and characterization of HUMSCs-Exos

Exosomes were isolated and purified from fresh or frozen cell culture supernatants (60). Briefly, the collected supernatant was centrifuged at 300*g*, 4 °C for 10 min to remove dead cells. The supernatant was then centrifuged at 10,000*g* for 30 min to remove smaller cell debris. The clarified supernatant was filtered through a 0.45 μm filter (Sartorius) and centrifuged at 120,000*g*, 4 °C for 70 min. Pellets were visible at the bottom of the centrifuge tube. The precipitates were resuspended in phosphate-buffered saline (PBS; Gibco) and centrifuged four times at 120,000*g* for 70 min each time. After discarding the supernatant, the pellets containing exosomes were collected. Finally, exosomes were resuspended in PBS and stored at −80 °C. The protein content of exosome suspensions was determined using the bicinchoninic acid protein assay kit (Beyotime). Western blotting was performed to detect the surface markers Cd 9, Cd 63, and Tsg 101 on exosomes. The morphology and size of exosomes were examined using TEM (Hitachi) and NTA (Zeta View PMX 120, Particle Matrix), respectively.

Primary OPCs culture

Isolation and culture of primary OPCs from rats (61). First, the cortices of neonatal Wistar rats were dissected within 72 h, and fresh cortical tissue was washed with Hank's Balanced Salt Solution (Yuanpei) to remove the vascular membrane. Subsequently, the tissue was cultured in Advanced D-MEM/F-12 (Dulbecco's modified Eagle Medium) medium (Invitrogen) containing 20% FBS. After 7 to 10 days, the clustered glial cells were mechanically oscillated for 18 to 20 h, and the cell suspension was collected and seeded into 6-well plates to obtain OPCs at a density of 300,000 cells per well. The purified OPCs

were cultured in serum-free proliferation medium, which consisted of D-MEM/F-12 supplemented with 10 ng/ml basic fibroblast growth factor (PeproTech), 20 ng/ml platelet-derived growth factor AA (PeproTech), 2% B27 (Thermo Fisher Scientific), and 1% N2 (Invitrogen). After 72 h of proliferation under these conditions, the cell culture medium was changed according to the experimental purpose and further cultured for an additional 48 h before collecting the cells for subsequent experiments. The control group was cultured in the abovementioned medium without the addition of PDGF and FGF, while the experimental group was cultured in the same medium but supplemented with HUMSCs-Exos instead of PDGF and FGF.

Animal experiment

Animal experimental procedures were approved by the Animal Research Committee of Shandong University Affiliated Shandong Provincial Hospital. The C57BL/6J male mice weighing approximately 25 g were used in this study. The animals were housed in standard microventilated isolator cages with a 12-h light/dark cycle. All mice were anesthetized by intraperitoneal injection of 4% chloral hydrate (400 mg/kg). To induce EAE, MOG 35 to 55 peptide (Sigma-Aldrich) was mixed with CFA [incomplete free adjuvant (Sigma-Aldrich) and *mycobacterium tuberculosis* (BD Difco)], followed by subcutaneous injection of 100ul on each side of the lower back of 6-week-old male C57BL/6J mice. Pertussis toxin (List Laboratories) at a dose of 200 ng was injected intraperitoneally into the mice on days 0 and 2 after immunization. Mice were weighed daily and assessed for clinical symptoms. Clinical scoring was performed on a scale of 0 to 5, where (0) represented no apparent changes, (1) indicated tail limpness without tail curling, complete tail paralysis, (2) represented slight hind limb paralysis, (2.5) indicated complete paralysis of one hind limb, (3) represented complete paralysis of both hind limbs, (3.5) indicated complete paralysis of both hind limbs and weakened forelimb strength, (4) represented complete paralysis, and (5) indicated death.

HUMSCs-Exos administration

First, OPCs were treated with different concentrations of HUMSCs-Exos for 48 h to determine the optimal concentration for exosome uptake. Based on Western blotting (Fig. 2*C*), 50 μg/ml was chosen as the optimal treatment concentration for the exosomes. Next, the incubation time for primary OPCs and exosomes was determined. Exosomes were labeled using the PKH67 staining kit (Sigma-Aldrich) following the manufacturer's instructions. The labeled exosomes (50 ug/ml) were diluted in the medium and incubated with OPCs for 0 or 48 h. Cells were fixed with 4% paraformaldehyde and subjected to immunostaining. Subsequently, lentiviral transduction of HUMSCs-Exos was performed. HUMSCs were cultured in 15 cm culture dishes (NEST Biotechnology) and transduced with Lv-miR-23a-3p (a lentiviral vector overexpressing miR-23a-3p) and Lv-NC (a lentiviral vector expressing a NC) (GenePharm). Cell culture supernatant was collected, and the modified HUMSCs-Exos overexpressing miR-23a-3p (Exos-Lv-miR23a-3p) were successfully isolated. These modified HUMSCs-Exos were added to OPCs at a concentration of 50 μg/ml and incubated for 48 h before being collected for subsequent experiments. In the *in vivo* experiment, EAE mice at the peak of disease were randomly divided into three groups: EAE + PBS group, EAE+HUMSCs-Exos group, and EAE+-modified HUMSCs-Exos (Exos-Lv-miR23a-3p) group (n = 10 mice per group). During the peak phase of EAE induction (day 14), mice in the experimental groups were intravenously injected with 25 μl PBS containing HUMSCs-Exos or modified HUMSCs-Exos (Exos-Lv-miR23a-3p) at a concentration of 50 μg. The control group mice received an injection of 25 μl PBS. Subsequently, the body weight and clinical scores of the mice were monitored daily. Until day 42, fresh brain tissue specimens were collected, and 4 μm-thick paraffin sections were prepared using standard methods. The paraffin sections were stained with LFB to evaluate the degree of demyelination.

Cell immunofluorescence

After fixing the cells with 4% paraformaldehyde, cell immunofluorescence staining was performed to identify primary OPCs and mature differentiated OLs. The cells (OPCs/OLs) were permeabilized with 0.1% Triton X-100 at room temperature for 10 min. The cells were blocked with 1% BSA for 30 min. Subsequently, the cells were incubated overnight at 4 °C with primary antibodies. The primary antibodies included platelet-derived growth factor receptor α (1:100), chondroitin sulfate proteoglycan 4 (NG2) (1:50) (Abcam), and Mbp (1 μg/ml) (Abcam). Next, the cells were incubated with appropriate FITC-conjugated secondary antibodies (Abcam). DAPI was added, and the cells were incubated at room temperature. The cells were observed under an inverted fluorescence microscope. The TUNEL assay (Boehringer Mannheim) was used for apoptosis detection in cells to analyze apoptotic cells *in situ*. TUNEL staining of OPCs was observed under a fluorescence microscope, and the percentage of TUNEL-positive (TUNEL+) cells relative to the total number of cells was determined by counting at least three random fields per coverslip.

MiRNA sequencing

Total RNA was extracted using TRIzol reagent (Invitrogen) following the manufacturer's instructions. Preparation of cDNA libraries included end-repairing small RNA and reverse transcription. Mature miRNA libraries were generated through 6% high-resolution polyacrylamide gel electrophoresis (Invitrogen). Quality control and quantification were performed on the sequencing libraries. Sequencing was carried out on the HiSeq 2500 platform (Illumina) to obtain raw small RNA sequence data from independent samples. The raw reads were filtered using the FASTX-Toolkit software (http://hannonlab.cshl.edu/fastx_toolkit/). MiRDeep2 software (https://www.mdc-berlin.de) was used to identify known miRNAs and their expression levels based on databases (62). Differential expression genes were determined and ranked from highest to lowest by selection. The miRanda software

(http://www.mocrorna.org) and TargetScan (http://www.targetscan.org) databases were used to predict and calculate the mRNA target genes for each miRNA.

RNA sequencing

Total RNA was extracted by TRIzol reagent. Subsequently, cDNA libraries were prepared and sequenced on the Illumina NovaSeq platform. DEGs were identified as genes with adjusted p value < 0.05 and log2 fold change > 1 or <-1. To assess the functional significance of DEGs, Gene Ontology, and Kyoto Encyclopedia of Genes and Genomes pathway enrichment analysis were performed using the R packages clusterProfiler and DAVID (http://david.ncifcrf.gov/).

Cell transfection

Primary OPCs were transfected with specific miRNA mimics, alongside a miRNA NC (JEKAIYER). Transfection was conducted 2 days after seeding the cells, employing Lipofectamine 2000 (Invitrogen) as per the manufacturer's guidelines. OPCs differentiation assay was initiated 6 h after transfection. qPCR was performed to validate the expression of transfected miRNA. The Tbr1 overexpression plasmid (Tbr1-OE) and NC were obtained from RiboBio company. According to the manufacturer's instructions, 1 to 2 μg of DNA was diluted in 200 μl Opti-MEM medium (Gibco), and then 2 μl of Neofect^{tm} DNA transfection reagent (Beijing) was added to the 6-well plate containing the cells. After 24 h of transfection, cells were collected and processed according to the experimental requirements. The Tbr1 levels between transfected cells and control cells were compared using Western blotting to validate the transfection efficiency.

Luciferase reporter assay

HEK293T cells were used for the luciferase reporter gene assay. Briefly, the 3′UTR of Tbr1 containing the predicted target site of miR-23a-3p was cloned into the pNGM-UTR dual-luciferase reporter gene vector (Promega) containing Renilla and firefly luciferase genes (internal controls). HEK293T cells were seeded in 96-well plates and cotransfected with 0.1 μg of luciferase reporter cells, along with miR-23a-3p mimics or NC at a concentration of 100 nM. After 48 h, the dual-luciferase reporter gene assay system (E1910; Promega) was used. According to the kit instructions, the relative luciferase activity (Renilla luciferase/firefly luciferase) was calculated to assess the regulatory effect of miR-23a-3p on its putative target gene Tbr1.

Quantitative PCR

Total RNA of cells was extracted using TRIzol reagent. The RNA was reverse transcribed into cDNA using the TaqMan MicroRNA Reverse Transcription Kit (Thermo Fisher Scientific). Subsequently, quantitative reverse transcription PCR was performed on the selected miRNAs using SYBR Green Premix Ex Taq polymerase (Takara). The cycle threshold (Ct) values were recorded for subsequent analysis (Ct value represents the number of reaction cycles required for the fluorescent signal to reach the set threshold in each reaction tube). The mRNA and miRNA expression levels were normalized to the expression levels of β-actin and U6, respectively, using the $2^{\wedge}$-ΔΔCT method.

qPCR primers sequences are as follows:

Mag: Forward-5′GATGCCCTCGTCCATCTCAG3′ , Reverse-5′ AAGCTCTCGTGGACCACTTG3′|

Mog: Forward-5′GTCTATCGGCGAGGGAAAGG3′ , Reverse-5′ AGCATAGGCACAAGGGCAAT3′|

Wnt5a: Forward-5′GCGGGACTTTCTCAAGGACA3′ , Reverse-5′ CGGCTGCCTATTTGCATCAC3′|

β-actin: Forward-5′CTTCCAGCCTTCCTTCCTGG3′ , Reverse-5′ AATGCCTGGGTACATGGTGG3′|

miR-23a-3p: Forward-5′GCGATCACATTGCCAGGG3′, Reverse-5′ AGTGCAGGGTCCGAGGTATT3′|

miR-146a-5p: Forward-5′CGCGTGAGAACTGAATTCCA3′, Reverse-5′AGTGCAGGGTCCGAGGTATT3′|

miR-122-5p: Forward-5′CGCGTGGAGTGTGACAATGG3′, Reverse-5′AGTGCAGGGTCCGAGGTATT3′|

miR-221-3p: Forward-5′ CGCGAGCTACATTGTCTGCTG. 3′, Reverse-5′ AGTGCAGGGTCCGAGGTATT3′|

miR-24-3P: Forward-5′GCGTGGCTCAGTTCAGCAG3′, Reverse-5′AGTGCAGGGTCCGAGGTATT3′|

miR-7a-5p: Forward-5′GCGCGTGGAAGACTAGTGATTT3′, Reverse-5′AGTGCAGGGTCCGAGGTATT3′|

U6: Forward-5′GTGCTCGCTTCGGCAGCACATAT3′, Reverse-5′AGTGCAGGGTCCGAGGTATT3′.

Western blotting

As previously described, total protein was obtained from the samples by lysing with radioimmunoprecipitation assay lysis buffer (Beyotime). The protein samples were separated using sodium dodecyl sulfate-polyacrylamide gel electrophoresis and then transferred onto a polyvinylidene fluoride membrane (Millipore). After blocking with 5% skim milk, the membrane was incubated with primary antibodies overnight at 4 °C, followed by incubation with horseradish peroxidase–conjugated secondary antibody. The primary antibodies used in this study included Mbp (1:1000), Mog (1:1000), Mag (1:1000), Tbr1 (1:1000) (Abcam), Akt (1:1000), Phospho-Akt (1:1000) (Cell Signaling Technology), Wnt7a/b (1:1000) (Santa Cruz Biotechnology), Wnt5a (1:500), β-Catenin (1:5000), Cd9 (1:1000), Cd81 (1:1000), Tsg101(1:2000), Gapdh (1:5000), α-Tubulin (1:2000) (Proteintech,). Marker proteins were detected using an enhanced chemiluminescence solution and a Bio-Rad imaging system (Bio-Rad). The band intensities were quantified for three independent experiments using Image J software.

Statistical analysis

All results were obtained from at least three independent experiments and are presented as mean ± standard error of the

mean (SEM). Quantitative data comparing the experimental group and the control group were analyzed using Student's *t* test, while multiple comparisons were performed using one-way analysis of variance (ANOVA) followed by Tukey's post hoc test. All statistical analyses were conducted using Prism 8 software (GraphPad), and statistical significance was considered when the *p*-value was less than 0.05.

Data availability

All the data described in the article are located within the article and/or its supporting information.

Supporting information—This article contains supporting information.

Acknowledgments—We would like to thank Shandong Provincial Hospital Central Laboratory for providing the experimental operating platform assistance.

Author contributions—D. Q. conceptualization; D. Q. methodology; D. Q. software; D. Q. data curation; D. Q. writing–original draft; C. W. writing–reviewing and editing; D. L. visualization; D. L. investigation; S. G. supervision.

Funding and additional information—These studies were supported by grant support from the National Natural Science Foundation of China (No. 82072079).

Conflict of interest—The authors declare that they have no conflict of interest with the contents of this article.

Abbreviations—The abbreviations used are: CNS, central nervous system; DEG, differentially expressed genes; EAE, experimental autoimmune encephalomyelitis; HUMSCs-Exos, exosomes derived from human umbilical cord mesenchymal stem cells; GO, Gene Ontology; KEGG, Kyoto Encyclopedia of Genes and Genomes; LFB, Luxol fast blue; Mag, myelin-associated glycoprotein; Mog, myelin oligodendrocyte glycoprotein; Mbp, myelin basic protein; MS, multiple sclerosis; MSC, mesenchymal stem cell; MSCs-Exos, MSCs-derived exosomes; NTA, nanoparticle tracking analysis; OL, oligodendrocyte; OPC, oligodendrocyte progenitor cell; PBS, phosphate-buffered saline; Pi3k, phosphoinositide 3-kinase; TEM, transmission electron microscopy.

References

1. Multiple sclerosis. *Nat. Rev. Dis. Primers* **4**, (2018), 44
2. Matute, C., and Perez-Cerda, F. (2005) Multiple sclerosis: novel perspectives on newly forming lesions. *Trends Neurosci.* **28**, 173–175
3. Correale, J., Gaitan, M. I., Ysrraelit, M. C., and Fiol, M. P. (2017) Progressive multiple sclerosis: from pathogenic mechanisms to treatment. *Brain* **140**, 527–546
4. Kuhlmann, T., Miron, V., Cui, Q., Wegner, C., Antel, J., and Bruck, W. (2008) Differentiation block of oligodendroglial progenitor cells as a cause for remyelination failure in chronic multiple sclerosis. *Brain* **131**, 1749–1758
5. Martin, I., Galipeau, J., Kessler, C., Le Blanc, K., and Dazzi, F. (2019) Challenges for mesenchymal stromal cell therapies. *Sci. Transl. Med.* **11**, eaat2189
6. Jadasz, J. J., Kremer, D., Gottle, P., Tzekova, N., Domke, J., Rivera, F. J., *et al.* (2013) Mesenchymal stem cell conditioning promotes rat oligodendroglial cell maturation. *PLoS One* **8**, e71814
7. Al Jumah, M. A., and Abumaree, M. H. (2012) The immunomodulatory and neuroprotective effects of mesenchymal stem cells (MSCs) in experimental autoimmune encephalomyelitis (EAE): a model of multiple sclerosis (MS). *Int. J. Mol. Sci.* **13**, 9298–9331
8. Xie, Q., Liu, R., Jiang, J., Peng, J., Yang, C., Zhang, W., *et al.* (2020) What is the impact of human umbilical cord mesenchymal stem cell transplantation on clinical treatment? *Stem Cell Res. Ther.* **11**, 519
9. Ha, D., Yang, N., and Nadithe, V. (2016) Exosomes as therapeutic drug carriers and delivery vehicles across biological membranes: current perspectives and future challenges. *Acta Pharm. Sin B* **6**, 287–296
10. Xu, M., Feng, T., Liu, B., Qiu, F., Xu, Y., Zhao, Y., *et al.* (2021) Engineered exosomes: desirable target-tracking characteristics for cerebrovascular and neurodegenerative disease therapies. *Theranostics* **11**, 8926–8944
11. Laso-Garcia, F., Ramos-Cejudo, J., Carrillo-Salinas, F. J., Otero-Ortega, L., Feliu, A., Gomez-de Frutos, M., *et al.* (2018) Therapeutic potential of extracellular vesicles derived from human mesenchymal stem cells in a model of progressive multiple sclerosis. *PLoS One* **13**, e0202590
12. Zhang, J., Zhang, Z. G., Lu, M., Zhang, Y., Shang, X., and Chopp, M. (2019) MiR-146a promotes oligodendrocyte progenitor cell differentiation and enhances remyelination in a model of experimental autoimmune encephalomyelitis. *Neurobiol. Dis.* **125**, 154–162
13. Martin, N. A., Molnar, V., Szilagyi, G. T., Elkjaer, M. L., Nawrocki, A., Okarmus, J., *et al.* (2018) Experimental demyelination and axonal loss are reduced in MicroRNA-146a deficient mice. *Front. Immunol.* **9**, 490
14. Lin, S. T., Huang, Y., Zhang, L., Heng, M. Y., Ptacek, L. J., and Fu, Y. H. (2013) MicroRNA-23a promotes myelination in the central nervous system. *Proc. Natl. Acad. Sci. U. S. A.* **110**, 17468–17473
15. Lin, S. T., and Fu, Y. H. (2009) miR-23 regulation of lamin B1 is crucial for oligodendrocyte development and myelination. *Dis. Model Mech.* **2**, 178–188
16. Qian, J., Zhai, A., Kao, W., Li, Y., Song, W., Fu, Y., *et al.* (2010) Modulation of miR-122 on persistently Borna disease virus infected human oligodendroglial cells. *Antivir. Res.* **87**, 249–256
17. Al-Ghezi, Z. Z., Miranda, K., Nagarkatti, M., and Nagarkatti, P. S. (2019) Combination of cannabinoids, Delta9- tetrahydrocannabinol and cannabidiol, ameliorates experimental multiple sclerosis by suppressing neuroinflammation through regulation of miRNA-mediated signaling pathways. *Front. Immunol.* **10**, 1921
18. Zhao, L., Yuan, Y., Li, P., Pan, J., Qin, J., Liu, Y., *et al.* (2018) miR-221-3p inhibits schwann cell myelination. *Neuroscience* **379**, 239–245
19. Wen, L. L., Yu, T. H., Ma, Y. Z., Mao, X. Y., Ao, T. R., Javed, R., *et al.* (2023) Sequential expression of miR-221-3p and miR-338-3p in Schwann cells as a therapeutic strategy to promote nerve regeneration and functional recovery. *Neural Regen. Res.* **18**, 671–682
20. Lei, C. J., Chen, W., Li, M. H., Xu, Y., Pan, Q. Y., Zheng, G., *et al.* (2020) MiR-24 inhibits oligodendrocyte precursor cell differentiation after spinal injury by targeting adrenal medulla. *Eur. Rev. Med. Pharmacol. Sci.* **24**, 2865–2873
21. Cai, S., Shi, G. S., Cheng, H. Y., Zeng, Y. N., Li, G., Zhang, M., *et al.* (2017) Exosomal miR-7 mediates bystander autophagy in lung after focal brain irradiation in mice. *Int. J. Biol. Sci.* **13**, 1287–1296
22. Adusumilli, L., Facchinello, N., Teh, C., Busolin, G., Le, M. T., Yang, H., *et al.* (2020) miR-7 controls the dopaminergic/oligodendroglial fate through Wnt/beta-catenin signaling regulation. *Cells* **9**, 711
23. Fazel Darbandi, S., Robinson Schwartz, S. E., Qi, Q., Catta-Preta, R., Pai, E. L., Mandell, J. D., *et al.* (2018) Neonatal Tbr1 dosage controls cortical layer 6 connectivity. *Neuron* **100**, 831–845 e7
24. Fazel Darbandi, S., Robinson Schwartz, S. E., Pai, E. L., Everitt, A., Turner, M. L., Cheyette, B. N. R., *et al.* (2020) Enhancing WNT signaling restores cortical neuronal spine maturation and synaptogenesis in Tbr1 mutants. *Cell Rep.* **31**, 107495
25. Caracci, M. O., Avila, M. E., Espinoza-Cavieres, F. A., Lopez, H. R., Ugarte, G. D., and De Ferrari, G. V. (2021) Wnt/beta-Catenin-Dependent transcription in autism spectrum disorders. *Front. Mol. Neurosci.* **14**, 764756
26. Mecha, M., Yanguas-Casas, N., Feliu, A., Mestre, L., Carrillo-Salinas, F. J., Riecken, K., *et al.* (2020) Involvement of Wnt7a in the role of M2c microglia in neural stem cell oligodendrogenesis. *J. Neuroinflam.* **17**, 88

27. Wang, L. P., Pan, J., Li, Y., Geng, J., Liu, C., Zhang, L. Y., *et al.* (2022) Oligodendrocyte precursor cell transplantation promotes angiogenesis and remyelination *via* Wnt/beta-catenin pathway in a mouse model of middle cerebral artery occlusion. *J. Cereb. Blood Flow Metab.* **42**, 757–770
28. Griveau, A., Seano, G., Shelton, S. J., Kupp, R., Jahangiri, A., Obernier, K., *et al.* (2018) A glial signature and Wnt7 signaling regulate glioma-vascular interactions and tumor microenvironment. *Cancer Cell* **33**, 874–889.e7
29. Chavali, M., Ulloa-Navas, M. J., Perez-Borreda, P., Garcia-Verdugo, J. M., McQuillen, P. S., Huang, E. J., *et al.* (2020) Wnt-dependent oligodendroglial-endothelial interactions regulate white matter vascularization and attenuate injury. *Neuron* **108**, 1130–11345.e5
30. Yuen, T. J., Silbereis, J. C., Griveau, A., Chang, S. M., Daneman, R., Fancy, S. P. J., *et al.* (2014) Oligodendrocyte-encoded HIF function couples postnatal myelination and white matter angiogenesis. *Cell* **158**, 383–396
31. Shimizu, T., Smits, R., and Ikenaka, K. (2016) Microglia-induced activation of non-canonical Wnt signaling aggravates neurodegeneration in demyelinating disorders. *Mol. Cell Biol.* **36**, 2728–2741
32. Momsen, A. H., Ortenblad, L., and Maribo, T. (2022) Effective rehabilitation interventions and participation among people with multiple sclerosis: an overview of reviews. *Ann. Phys. Rehabil. Med.* **65**, 101529
33. Allegretta, C., D'Amico, E., Manuti, V., Avolio, C., and Conese, M. (2022) Mesenchymal stem cell-derived extracellular vesicles and their therapeutic use in central nervous system demyelinating disorders. *Int. J. Mol. Sci.* **23**, 3829
34. Yousefi, F., Lavi Arab, F., Saeidi, K., Amiri, H., and Mahmoudi, M. (2019) Various strategies to improve efficacy of stem cell transplantation in multiple sclerosis: focus on mesenchymal stem cells and neuroprotection. *J. Neuroimmunol.* **328**, 20–34
35. Rivera, F. J., and Aigner, L. (2012) Adult mesenchymal stem cell therapy for myelin repair in multiple sclerosis. *Biol. Res.* **45**, 257–268
36. Shen, Z., Huang, W., Liu, J., Tian, J., Wang, S., and Rui, K. (2021) Effects of mesenchymal stem cell-derived exosomes on autoimmune diseases. *Front. Immunol.* **12**, 749192
37. Sun, Y., Liu, G., Zhang, K., Cao, Q., Liu, T., and Li, J. (2021) Mesenchymal stem cells-derived exosomes for drug delivery. *Stem Cell Res. Ther.* **12**, 561
38. Xian, P., Hei, Y., Wang, R., Wang, T., Yang, J., Li, J., *et al.* (2019) Mesenchymal stem cell-derived exosomes as a nanotherapeutic agent for amelioration of inflammation-induced astrocyte alterations in mice. *Theranostics* **9**, 5956–5975
39. Li, Z., Liu, F., He, X., Yang, X., Shan, F., and Feng, J. (2019) Exosomes derived from mesenchymal stem cells attenuate inflammation and demyelination of the central nervous system in EAE rats by regulating the polarization of microglia. *Int. Immunopharmacol.* **67**, 268–280
40. Oveili, E., Vafaei, S., Bazavar, H., Eslami, Y., Mamaghanizadeh, E., Yasamineh, S., *et al.* (2023) The potential use of mesenchymal stem cells-derived exosomes as microRNAs delivery systems in different diseases. *Cell Commun. Signal.* **21**, 20
41. Gu, S., Jin, L., Zhang, F., Sarnow, P., and Kay, M. A. (2009) Biological basis for restriction of microRNA targets to the 3' untranslated region in mammalian mRNAs. *Nat. Struct. Mol. Biol.* **16**, 144–150
42. Friedman, T. N., Yousuf, M. S., Catuneanu, A., Desai, M., Juzwik, C. A., Fournier, A. E., *et al.* (2019) Profiling the microRNA signature of the peripheral sensory ganglia in experimental autoimmune encephalomyelitis (EAE). *J. Neuroinflam.* **16**, 223
43. Murugaiyan, G., da Cunha, A. P., Ajay, A. K., Joller, N., Garo, L. P., Kumaradevan, S., *et al.* (2015) MicroRNA-21 promotes Th17 differentiation and mediates experimental autoimmune encephalomyelitis. *J. Clin. Invest.* **125**, 1069–1080
44. Martin, N. A., Hyrlov, K. H., Elkjaer, M. L., Thygesen, E. K., Wlodarczyk, A., Elbaek, K. J., *et al.* (2020) Absence of miRNA-146a differentially alters microglia function and proteome. *Front. Immunol.* **11**, 1110
45. Vistbakka, J., Sumelahti, M. L., Lehtimaki, T., and Hagman, S. (2022) Temporal variability of serum miR-191, miR-223, miR-128, and miR-24 in multiple sclerosis: a 4-year follow-up study. *J. Neurol. Sci.* **442**, 120395
46. Galloway, D. A., Blandford, S. N., Berry, T., Williams, J. B., Stefanelli, M., Ploughman, M., *et al.* (2019) miR-223 promotes regenerative myeloid cell phenotype and function in the demyelinated central nervous system. *Glia* **67**, 857–869
47. Gaesser, J. M., and Fyffe-Maricich, S. L. (2016) Intracellular signaling pathway regulation of myelination and remyelination in the CNS. *Exp. Neurol.* **283**, 501–511
48. Mathews, E. S., and Appel, B. (2016) Cholesterol biosynthesis supports myelin gene expression and axon ensheathment through modulation of P13K/Akt/mTor signaling. *J. Neurosci.* **36**, 7628–7639
49. Tanga, N., Kuboyama, K., Kishimoto, A., Kiyonari, H., Shiraishi, A., Suzuki, R., *et al.* (2019) The PTN-PTPRZ signal activates the AFAP1L2-dependent PI3K-AKT pathway for oligodendrocyte differentiation: targeted inactivation of PTPRZ activity in mice. *Glia* **67**, 967–984
50. Gomez, O., Sanchez-Rodriguez, A., Le, M., Sanchez-Caro, C., Molina-Holgado, F., and Molina-Holgado, E. (2011) Cannabinoid receptor agonists modulate oligodendrocyte differentiation by activating PI3K/Akt and the mammalian target of rapamycin (mTOR) pathways. *Br. J. Pharmacol.* **163**, 1520–1532
51. Xiao, Q., Chen, Z., Jin, X., Mao, R., and Chen, Z. (2017) The many postures of noncanonical Wnt signaling in development and diseases. *Biomed. Pharmacother.* **93**, 359–369
52. Prasad, C. P., Chaurasiya, S. K., Guilmain, W., and Andersson, T. (2016) WNT5A signaling impairs breast cancer cell migration and invasion *via* mechanisms independent of the epithelial-mesenchymal transition. *J. Exp. Clin. Cancer Res.* **35**, 144
53. Zhang, C. J., Zhu, N., Liu, Z., Shi, Z., Long, J., Zu, X. Y., *et al.* (2020) Wnt5a/Ror2 pathway contributes to the regulation of cholesterol homeostasis and inflammatory response in atherosclerosis. *Biochim. Biophys. Acta Mol. Cell Biol. Lipids* **1865**, 158547
54. Gonzalez, P., Gonzalez-Fernandez, C., and Javier Rodriguez, F. (2021) Effects of Wnt5a overexpression in spinal cord injury. *J. Cell Mol. Med.* **25**, 5150–5163
55. Bulfone, A., Wang, F., Hevner, R., Anderson, S., Cutforth, T., Chen, S., *et al.* (1998) An olfactory sensory map develops in the absence of normal projection neurons or GABAergic interneurons. *Neuron* **21**, 1273–1282
56. Mendez-Gomez, H. R., Vergano-Vera, E., Abad, J. L., Bulfone, A., Moratalla, R., de Pablo, F., *et al.* (2011) The T-box brain 1 (Tbr1) transcription factor inhibits astrocyte formation in the olfactory bulb and regulates neural stem cell fate. *Mol. Cell Neurosci.* **46**, 108–121
57. Bejoy, J., Song, L., Zhou, Y., and Li, Y. (2018) Wnt/yes-associated protein interactions during neural tissue patterning of human induced pluripotent stem cells. *Tissue Eng. Part A.* **24**(7-8), 546–558
58. Yu, F., Weng, J., Yuan, Y. S., Kou, Y. H., Han, N., Jiang, B. G., *et al.* (2018) Wnt5a affects schwann cell proliferation and regeneration *via* Wnt/c-Jun and PTEN signaling pathway. *Chin Med. J. (Engl)* **131**, 2623–2625
59. Zhao, C. G., Qin, J., Li, J., Jiang, S., Ju, F., Sun, W., *et al.* (2021) LINGO-1 regulates Wnt5a signaling during neural stem and progenitor cell differentiation by modulating miR-15b-3p levels. *Stem Cell Res. Ther.* **12**, 372
60. Li, P., Kaslan, M., Lee, S. H., Yao, J., and Gao, Z. (2017) Progress in exosome isolation techniques. *Theranostics* **7**, 789–804
61. Chen, Y., Balasubramaniyan, V., Peng, J., Hurlock, E. C., Tallquist, M., Li, J., *et al.* (2007) Isolation and culture of rat and mouse oligodendrocyte precursor cells. *Nat. Protoc.* **2**, 1044–1051
62. Friedlander, M. R., Mackowiak, S. D., Li, N., Chen, W., and Rajewsky, N. (2012) miRDeep2 accurately identifies known and hundreds of novel microRNA genes in seven animal clades. *Nucleic Acids Res.* **40**, 37–52